SUBORDINATED ADVECTION-DISPERSION EQUATION FOR CONTAMINANT TRANSPORT

Boris Baeumer[1], David A. Benson[2], Mark M. Meerschaert[3], and Stephen W. Wheatcraft[1]

[1]Department of Geologic Sciences, University of Nevada, Reno, NV 89557

[2]Desert Research Institute – Division of Hydrologic Sciences, Reno, NV 89512

[3]Department of Mathematics, University of Nevada, Reno, NV 89557

ABSTRACT

A mathematical method called subordination broadens the applicability of the classical advection--dispersion equation for contaminant transport. In this method, the time variable is randomized to represent the operational time experienced by different particles. In a highly heterogeneous aquifer, the operational time captures the fractal properties of the medium. This leads to a simple, parsimonious model of contaminant transport that exhibits many of the features (heavy tails, skewness, and non-Fickian growth rate) typically seen in real aquifers. We employ a stable subordinator that derives from physical models of anomalous diffusion involving fractional derivatives. Applied to a one-dimensional approximation of the MADE-2 data set, the model shows excellent agreement.

1. INTRODUCTION

The traditional advection—dispersion equation is a standard model for contaminant transport. The concentration profile for an ensemble of particles governed by this model will realize the probability distribution of a Brownian motion with drift. These Gaussian concentration profiles are symmetric, spread out from the center at a rate proportional to the square root of time, and have tails that diminish rapidly as one moves further away from the center. On the other hand, many tracer tests produce concentration profiles that are highly skewed and spread out from the center faster than the square root of time (super-diffusion), with heavy tails. Some authors have proposed multi-modal extensions of the advection—dispersion equation [*van Genuchten and Wierenga, 1976; Brusseau, 1992; Haggerty and Gorelick, 1995*] in which the aquifer is partitioned into mobile and immobile phases, in order to capture this non-Fickian behavior. This simplest 2-mode Gaussian model is not general enough to predict breakthrough curves in many tests [*Haggerty et al., 1999*].

We propose an extension of the advection-dispersion equation based on the idea of subordination, in which the time variable is randomized to represent the operational time experienced by an individual tracer particle. On a small scale, the particle experiences classical advection and dispersion, but the rate at which advection and dispersion takes place varies as the particle samples more of the heterogeneous aquifer. This results in an average velocity that grows with time, leading to super-diffusion and heavy power-law tails. The specific randomization of mean velocity also results in skewed concentration profiles, as particles that experience a preponderance of high velocities travel much farther than the mean.

Many recent physical models of super-diffusion involve fractional derivatives [*Compte, 1997; Saichev and Zaslavsky, 1997; Chaves, 1998*], so that this process is also known as fractional diffusion. A linear advection — fractional dispersion equation has recently been developed [*Benson, 1998; Meerschaert, et al., 1999; Schumer, et al., 2000*] which combines fractional diffusion with linear advection. The subordination model considered here is governed by a fractional partial differential equation that includes fractional advection and dispersion. This fractional model is obtained from classical advection—dispersion through a specific operational time called the stable subordinator. Subordination is a standard tool in the theory of Markov and Lévy processes [*e.g., Feller, 1971; Sato, 1999; Bertoin, 1996*]. Applying the stable subordinator to classical diffusion yields fractional diffusion. We subordinate both advection and dispersion, so that physically a particle moves through a random accumulation of small samples in which the advection—dispersion equation is locally valid. Eventually, the particle samples more of the variation in an aquifer, moving through both high and low velocity zones, resulting in a more realistic model of contaminant transport.

2. SUBORDINATION

The classical one—dimensional advection—dispersion equation (ADE):

$$\frac{\partial C(x,t)}{\partial t} = -v\frac{\partial C(x,t)}{\partial x} + D\frac{\partial^2 C(x,t)}{\partial x^2};\ C(x,0) = \delta(x) \tag{1}$$

describes the evolution of a tracer plume injected at location $x = 0$ at time $t = 0$, where v represents the advective velocity, and D the combined effects of molecular diffusion and advective dispersion. The solution $C(x,t) = N(x \mid vt, 2Dt)$, where

$$N(x \mid m, s^2) = \frac{1}{\sqrt{2p\,s^2}} \exp\left[\frac{(x-m)^2}{2s^2}\right] \tag{2}$$

is the normal density with mean m and standard deviation s. We may consider $C(x,t)$ as the probability density of the random variable $X(t)$, which represents the location of a random tracer particle at time t; then the stochastic process $\{X(t) : t \geq 0\}$ is a Brownian motion with drift. This stochastic model is justified by the central limit theorem, which states that sums of many finite—variance random particle jumps will converge to a normal distribution. The problem with this classical model is that tracer plumes often behave differently than a Brownian motion with drift. Many tracer plumes are skewed instead of symmetric, and they spread faster than the square root of time, i.e., $\sigma_{X(t)} \propto t^{\gamma}$, where g > ½, mainly in the downstream direction.

We propose a modification of the standard advection—dispersion equation that takes into account the effects of heterogeneous media. In real aquifers, tracer particles are subject to dispersion by differential advection, which causes the tracer plume to spread out as different particles experience different advective velocities. As particles sample more of the heterogeneity of the medium, the velocity contrasts tend to increase. Our model, based on the principle of *subordination* [*Bochner, 1955; Feller, 1971; Bertoin, 1996; Sato, 1999*], recognizes this cumulative effect. Since different particles experience different velocities, it is as if time passes more quickly for some particles than for others. Those particles in high velocity zones experience more intense effects of both advection and dispersion. We can represent this effect by the application of *operational time.* The subjective or operational time experienced by each particle is the cumulative effect of transitions between high and low velocity zones, represented by a random time $T(t)$. Hence, in our model the random particle location at time t is given by the subordinated Brownian motion $X(T(t))$ [*Bochner, 1955; Feller, 1971; Sato, 1999*].

In a completely homogeneous aquifer, the operational time $T(t) = t$ for every particle, and our model reduces to the classical ADE. In the transfer function [*Jury, 1982*] or "stream tube" [*Cvetkovic and Dagan, 1994*] models, the operational time $T(t) = Zt$ where Z is a random variable which governs the (constant in time) velocity of a randomly chosen particle, often assumed to be lognormal [*Jury, 1982*]. In a heterogeneous aquifer, the random time process should reflect the fact that a particle's speed is not constant. One can model the random time process so that it represents some fractal properties of the medium. A simple stochastic process that respects these fractal properties is a *Lévy motion* $\{Y(t) : t \geq 0\}$, a stochastic process with stationary independent increments such that the density of the random variable $Y(t)$ has Fourier transform $\exp(-Bt\,|k|^{a})$ for some $0 < a \leq 2$. The sample paths of a Lévy motion with index a are random fractals with dimension a [*Taylor, 1986*]. Lévy motions are used in physics as a model for *anomalous diffusion* (for a comprehensive review article, see [*Klafter et al., 1996*]). The special case $a = 2$ is the usual Brownian motion model for diffusion. All the other symmetric Lévy motions are subordinated Brownian motion without drift $X(T(t))$ whose operational time is given by a stochastic process $\{T(t): t \geq 0\}$ with stationary independent increments, independent of the Brownian motion, such that the density $g(s\,|\,t)$ of the random variable $T(t)$ has Laplace transform $\exp(-ts^{a/2})$. For a visualization of the $a/2$-stable densities $g(s\,|\,1) = t^{2/a} g(st^{2/a}\,|\,t)$, see Fig. 1. This particular choice of $g(s\,|\,t)$ is called the *stable subordinator*, since in this case the random particle location $X(T(t))$ has a *stable distribution* [*Feller, 1971*]. We adopt this formula for operational time, but we subordinate a Brownian motion with drift in order to include the effects of both advection and diffusion/dispersion. In this model, particles always undergo Fickian "local" dispersion, but they also experience variability in the mean velocity along a trajectory.

The solution $C(x,t) = N(x\,|\,vt, 2Dt)$ to (1) represents the family of probability densities for a Brownian motion with drift $\{X(t): t \geq 0\}$. A simple conditioning argument shows that

$$C_S(x,t) = \int_0^\infty N(x\,|\,vs, 2Ds)\, g(s\,|\,t)\, ds \tag{3}$$

defines the family of probability densities for the subordinated Brownian motion with drift $\{X(T(t)): t \geq 0\}$. How random time translates into random velocity distribution is seen by a change of variables:

$$C_S(x,t) = \int_0^\infty N(x\,|\,ut, \frac{2Du}{v} t)\, g(ut/v\,|\,t)\, t/v\, du \tag{4}$$

The variable u in (4) represents the different local velocities that particles experience as they travel, because when the operational time *T(t)=s,* particles travel an average distance $ut = vs$

in time t. A simple change of variables shows that the term $g(ut/v\,|\,t)t/v$ is the probability density of the local velocities *T(t)v/t*. Since *T(t)* has Laplace transform $\exp(-ts^{a/2})$ it is easy to check that *T(t)* is identically distributed with $t^{2/a}T(1)$. Hence, the local velocities are identically distributed with $t^{2/a-1}T(1)v$, which tends to increase with time in the case $a<2$ corresponding to anomalous diffusion. Furthermore, this implies that the dimensions of v have to satisfy $[T]^{2/a-1}[v]=[L]/[T]$, or $[v]=[L]/[T]^{2/a}$. A similar argument shows that the average local plume standard deviation $s_{X(t)}$ is identically distributed with $t^{1/a}\sqrt{2DT(1)}$. Thus, the plume spreads faster than $t^{1/2}$ and $[D]=[L]^2/[T]^{2/a}$.

Kanter [1975] developed an analytic formula for the stable subordinator $g(s\,|\,t)$ that allows us to compute $C_S(x,t)$ directly. In this case, Bochner [1949] argued that $C_S(x,t)$ solves the fractional partial differential equation

$$\frac{\partial C_S(x,t)}{\partial t}=-\left(v\frac{\partial}{\partial x}-D\frac{\partial^2}{\partial x^2}\right)^{a/2}C_S(x,t);\; C_S(x,0)=d(x) \qquad (5)$$

which reduces to (1) if $a=2$. Balakrishnan [1960] carefully defined and studied these fractional powers of linear operators (such as the differential operator in (5)). The Fourier transform of the fractional operator in this case would be given as $-\left(vik+Dk^2\right)^{a/2}$. In the pure diffusion case where v = 0, the normal density $N(x\,|\,vs,2Ds)$ has Fourier transform $\exp[-s(k^2D)]$ so that (3) reduces to $\exp[-t(k^2D)^{a/2}]=\exp(-tB|\,k\,|^a)$ using the formula for the Laplace transform of $g(s\,|\,t)$. Hence, $C_S(x,t)$ describes a symmetric Lévy motion with index a, which is the solution to (5) in the special case v = 0.

Clearly, the notion of operational time is not limited to the one-dimensional case. Extensions to 3-D with different boundary and initial conditions are straightforward, since the solutions are given as a transform of the readily available solutions to the classical problem. In short, if $C(\vec{x},t)$ is the solution to the problem with $a = 2$, then $C_S(\vec{x},t) = \int_0^\infty C(\vec{x},s)g(s\,|\,t)ds$ is the solution to the subordinated problem.

3. PROPERTIES OF THE MODEL

In this section we establish some properties of the subordinated Brownian motion model that can be empirically verified for field data. We consider peak concentration, plume tail behavior, and the observed mean and variance in the case of the stable subordinator. The peak value of a plume described by this model decays at a rate between $t^{-1/a}$ and $t^{-2/a}$. If v=0, then the solution $C_S(x,t)$ to (5) is a symmetric Lévy motion with Fourier transform $\exp(-tD^{a/2}\,|\,k\,|^a)$. Thus, $C_S(x,t) = \frac{1}{t^{1/a}D^{1/2}} f_a\left(\frac{x}{t^{1/a}D^{1/2}}\right)$, where the Fourier transform of $f_a(x)$ is $\exp(-\,|\,k\,|^a)$. Therefore, the peak value decays proportional to $t^{-1/a}$. If D=0, the solution is a completely skewed Lévy motion; i.e., its Fourier transform is given by $\exp[-tv^{a/2}(ik)^{a/2}]$. Thus, $C_S(x,t) = \frac{1}{t^{2/a}v} g_a\left(\frac{x}{t^{2/a}v}\right)$, where the Fourier transform of g_a is $\exp[-(ik)^{a/2}]$ (See Fig. 1 for graphs of $g_a(s) = g(s\,|\,1)$ for different a.) Therefore, in this case, the peak value decays like $t^{-2/a}$. For the general case, there is no analytical solution, so we rely on a numerical integration. We used an adaptive Simpson's Rule to approximate the first integral in formula (3). The stable subordinator $g(s\,|\,t) = t^{-2/a} g(st^{-2/a}\,|\,1)$ where $g(s\,|1)$ was computed using the formula [*Kanter, 1975*]

$$g(s\,|\,1) = \begin{cases} \left(\frac{1}{p}\right)\cdot\left(\frac{a}{2-a}\right)\cdot\left(\frac{1}{s}\right)^{\frac{2}{2-a}} \int_0^p a(u)\exp\left[-a(u)s^{\frac{a}{a-2}}\right]du \\ \text{where } \; a(u) = \left[\frac{\sin\,(a\,u/2)}{\sin\,(u)}\right]^{\frac{2}{2-a}} \frac{\sin\left[(1-a/2)u\right]}{\sin\,(a\,u/2)} \end{cases}$$

for $s < 2$ and

$$g(s\,|\,1) = \sum_{k=0}^{\infty} \frac{-\Gamma(ka\,/\,2+1)}{psk!}\left[-(s)^{-a/2}\right]^k \sin(pka\,/\,2)$$

for $s \geq 2$ [*Feller, 1971*]. The resulting simulation shows that peak concentration falls off at a rate between $t^{-1/a}$ and $t^{-2/a}$, depending on the dispersivity D/v.

Next we consider the behavior of the plume tails. For our model, a simple analytical argument (Appendix) shows that the leading tail falls off like a power law

$$C(x,t) \approx \frac{a}{2}\frac{|v|^{a/2}\,t}{\Gamma(1-a\,/2)}\,x^{-a\,/2-1} \quad \text{as} \quad x \to \infty, \tag{5}$$

where $f(x) \approx g(x)$ means that $f(x)/g(x) \to 1$. A log—log plot of concentration versus distance should show a straight line with slope $-a\,/2-1$ on the leading (downstream) tail. For $v \neq 0$ one can show that the trailing tail decays at least exponentially, so that the leading tail dominates.

The theoretical mean and variance of concentration $C(x,t)$ are improper integrals

$$m(t) = \int_{-\infty}^{\infty} xC(x,t)dx \quad \text{and} \quad s^{\,2}(t) = \int_{-\infty}^{\infty}\left[x - m(t)\right]^2 C(x,t)dx\,. \tag{5a}$$

Because the concentration $C(x,t)$ has power law tails, these integrals do not exist mathematically, meaning that in practice they will grow with scale and do not converge to a fixed value. When the mean and variance of a plume are estimated from field data, we only use a finite number of observations from a fixed well field, and we cannot observe concentrations below detection limits. This is mathematically equivalent to estimating the *observed* mean and variance

$$m_{obs}(t) = \int_0^L xC(x,t)dx \quad \text{and} \quad s^2_{obs}(t) = \int_0^L [x - m_{obs}(t)]^2 C(x,t)dx . \tag{5b}$$

where L represents the distance from the injection point to the farthest downstream well at which tracer is detected. An analytical argument (Appendix) shows that $m_{obs}(t) \approx c_1 t L^{1-a/2}$ and $s^2_{obs}(t) \approx c_2 t L^{2-a/2}$ for $t^{2/a} << L$, where

$$c_1 = \frac{a}{2-a}\frac{|v|^{a/2}}{\Gamma(1-a/2)} \quad \text{and} \quad c_2 = \frac{a}{4-a}\frac{|v|^{a/2}}{\Gamma(1-a/2)} . \tag{5c}$$

Notice that (5c) does not collapse to the normal case for $a = 2$. This is due to the fact that we only have heavy tails for $a < 2$. The detection length L provides a useful scale for dimensional analysis. Because of the fractal nature of the medium, the proper scaling is nonstandard. The *fractal* mean and variance, which depend on the observation scale, $m_0(t) = m_{obs}(t)/L^{1-a/2} \approx c_1 t$ and $s^2_0(t) = s^2_{obs}(t)/L^{2-a/2} \approx c_2 t$, grow linearly with time. A plot of the fractal mean or variance versus time should resemble a straight line whose slope depends on v and a according to formula (5c).

4. APPLICATION

The Macro Dispersion Experiment (MADE) site is located on the Columbus Air Force Base in northeastern Mississippi. The unconfined, alluvial aquifer consists of generally unconsolidated sands and gravel with smaller clay and silt components and is highly heterogeneous [*Rehfeldt et al., 1992; Boggs and Adams, 1992, Boggs et al., 1993*]. Irregular lenses and horizontal layers were observed in an aquifer exposure near the site [*Rehfeldt et al., 1992*]. Detailed studies characterizing the spatial variability of the aquifer and the spreading of the conservative tracer plume for the experiment conducted between October 1986 and June 1988 (MADE-1) are summarized by Boggs and Adams [1992], Adams and Gelhar [1992], and Rehfeldt et al. [1992]. Adams and Gelhar [1992] documented the dramatically non-Gaussian behavior and anomalous spreading of the plume. A synopsis of the second experiment (MADE-2), conducted between June 1990 and September 1991, is given by Boggs et al. [1993].

We fit our subordination model to the MADE-2 tritium tracer data using the results of Section 3. Since the observed center of mass of the plume, upon scaling by the observation scale, should follow a straight line, we project onto this axis of flow to obtain a one-dimensional model in space. At each point along this line we take concentration to be the maximum observed value. Since the spreading in the transverse and vertical directions is basically uniform over the length of the plume, the normalization of the concentration profile to 100% mass recovery adjusts the values for the lateral spreading. In Section 3 we showed that the leading tail of the model plume decays like $x^{-1-a/2}$. Figure 2 shows that for the MADE-2 data, the leading tail resembles a power law of order $x^{-1.7}$, which supports a fractional order approach and leads to an estimate $a = 1.4$ for the fractal index. Next we calculate the observed mean and variance using trapezoidal integration on the one-dimensional concentrations. Both the observed mean and variance grow faster than linearly with time. Following the procedure detailed in Section 3, we then compute the fractal mean and variance by rescaling according to the detection length *L*, which we take to be the distance downstream to the furthest measured concentration, so that *L* grows with time. The resulting fractal mean and variance plotted in Figures 3 and 4 grows linearly with time, which also supports the subordination approach and leads to an estimate for the velocity parameter v. Linear regression yields slopes of m_1=0.0156 and m_2=0.0037 respectively. Using (5c) we obtain

$v = \left[\frac{m_1(2-a)\Gamma(1-a/2)}{a}\right]^{2/a} = .0037 m/d^{2/1.4}$, and

$v = \left[\frac{m_2(4-a)\Gamma(1-a/2)}{a}\right]^{2/a} = .0039 m/d^{2/1.4}$, respectively. We use $v = .0039 m/d^{2/1.4}$ in our model. Finally, we obtain the estimate $D = 0.0022 m^2/d^{2/1.4}$ for the dispersion parameter by fitting our model to the one-dimensional concentration data, normalized to constant total mass (by using maximum values on the projected axis of flow we found a mass recovery of 100%, 100%, 98% and 75% for the four snapshots). In particular, we minimize the sum of the squared difference between the logarithms of the predicted and observed concentrations (a measure of relative error) for the last three snapshots (elapsed times of 132, 224, and 328 days). Figures 5 and 6 show the resulting model concentrations together with the plume data. The concentration curves were obtained from equation (3) by numerical integration, using the method described in Section 3. We judge the fit to be adequate, and we conclude that our subordinated Brownian motion model captures the most important features of the MADE-2 tritium plume.

5. DISCUSSION

We propose an extension to the classical advection—dispersion equation for solute transport using operational time. Our model recognizes that particles sample more of the variability in the aquifer with time. The resulting stochastic process model is a subordinated Brownian motion with drift. The stable subordinator we use to model operational time describes the instantaneous (local) particle velocities. The resulting concentration plumes exhibit the heavy leading tails and nonlinear growth of observed variance typically associated with anomalous diffusion. These features are also commonly observed in real plumes, particularly those in heterogeneous media. The model does not predict a heavy trailing tail that is sometimes observed. One might have to invoke mass exchange with non-flowing regions or allow for infinite mean waiting times in order to capture this phenomenon. As in Brownian motion we have an infinite speed of propagation. It is important to keep in mind that this is an ergodic model, and as the plume samples more and more of the heterogeneity, the plume will approach the ergodic state.

Subordination is a method that can also be applied to 3-D problems with various boundary conditions. We support our model using the MADE-2 tritium plume data, resulting in the predicted concentrations shown in Figures 5 and 6. These curves faithfully reproduce the most important features of the plume data, using a computationally efficient model involving very few parameters. The question of how to estimate those parameters *a priori* is still not solved in a satisfactory fashion. Can a be estimated using the *K* distribution? Can we estimate the fractal moments in a different way? Can we estimate the uncertainty/variability in plume position? These are left as open questions.

The classical Brownian motion with drift emerges as a special case of our model, when the operational time is the same for all particles. When operational time is given in terms of a random velocity, we obtain a variant of the "streamtube" model (e.g., Jury, [1982]; Cvetkovic and Dagan, [1994]). The difference between our model and theirs is that we allow the probability distribution of the velocity for each individual particle to vary over time according to an ergodic limit theorem, whereas the streamtube model varies the velocities in space according to given soil properties.

Another related model is the fractional advection—dispersion equation [*Benson,* 1998, *Benson et al.* 2000 a,b,c]. In the case of symmetric plumes, their equation is equivalent to subordination of pure diffusion, together with a moving coordinate system to handle the advection. Their equation was also used to model the MADE-2 plume [*Benson, et al. 2000a*] and the quality of the fit was similar to Figures 5 and 6. Their estimation of $a = 1.1$ is lower compared to ours mainly due to the fact that in their model the heavy tails are entirely produced by fractional dispersion, whereas in our model the main culprit is fractional advection.

Models incorporating mass exchange between flowing and stagnant regions have also been able to predict aspects of the MADE data [*Harvey and Gorelick, 2000*]. In particular they give a nice explanation why the total solute mass reported at early times [*Adams and Gelhar, 1992; Boggs et al., 1993; Boggs and Adams, 1992*], is higher than the mass injected and why there is a significant loss of mass at later times. They also predict skewness in the plume; however, the models inherently fail to predict the observed power-law leading tail (Fig. 2).

The dual-domain models represent the particle velocity pdf by 2 Gaussian modes (one of the advective-dispersive phase and a second zero-mean velocity diffusion phase). The present subordinated model, like the streamtube models, explicitly represents the entire velocity pdf. The stable subordinator captures the high velocities, via the power-law tail, and the high degree of skewness. Our choice of the subordinator is implied by limit theorems and solves a fractional-order PDE. Other site-specific subordinators could be easily implemented.

Appendix

The density $g(s|1)$ with Laplace transform $\exp(-l^{a/2})$ is the density of a completely positively skewed $a/2$-stable distribution and has a heavy leading tail decaying like $g(s|1) \approx \frac{a}{2} g_a s^{-1-a/2}$, where $g_a = 1/\Gamma(1-a/2)$ (see, for example, Samorodnitsky and Taqqu, [1994]). Thus, $g(s|t) = t^{-2/a} g(st^{-2/a},1) \approx \frac{a}{2} g_a t s^{-1-a/2}$. Since for ε>0, on one hand,

$$\int_x^\infty \int_0^\infty g(s|t) N(h|vs,2Ds) ds dh = \int_0^\infty g(s|t) \int_x^\infty N(h|vs,2Ds) dh ds$$

$$= \int_0^{\frac{x}{(1-e)v}} g(s|t) \int_x^\infty N(h|vs,2Ds) dh ds + \int_{\frac{x}{(1-e)v}}^\infty g(s|t) \int_x^\infty N(h|vs,2Ds) dh ds$$

$$\geq \int_{\frac{x}{(1-e)v}}^\infty g(s|t) \int_x^\infty N(h|x/(1-e),2Dx/v(1-e)) dh ds$$

$$= \frac{1}{2} \operatorname{erfc}\left[\frac{-ex}{\sqrt{4Dx(1-e)/v}}\right] \int_{\frac{x}{(1-e)v}}^\infty g(s|t) ds \approx g_a t \left[\frac{x}{(1-e)v}\right]^{-a/2},$$

and on the other hand,

$$\int_x^\infty \int_0^\infty g(s|t) N(h|vs,2Ds) ds dh = \int_0^\infty g(s|t) \int_x^\infty N(h|vs,2Ds) dh ds$$

$$= \int_0^{\frac{x}{(1+e)v}} g(s|t) \int_x^\infty N(h|vs,2Ds) dh ds + \int_{\frac{x}{(1+e)v}}^\infty g(s|t) \int_x^\infty N(h|vs,2Ds) dh ds$$

$$\leq \int_0^{\frac{x}{(1+e)v}} \sup\left[g(s|t)\right] \int_x^\infty N(h|vs,2Ds) dh ds + \int_{\frac{x}{(1+e)v}}^\infty g(s|t)(1) ds$$

$$\leq \int_0^{\frac{x}{(1+e)v}} \sup\left[g(s\,|\,t)\right]\int_x^{\infty} N\left[h\,|\,x/(1+e),2Dx/(1+e)v\right]dh\,ds + \int_{\frac{x}{(1+e)v}}^{\infty} g(s\,|\,t)(1)ds$$

$$= \frac{x\sup\left[g(s\,|\,t)\right]}{(1+e)v}\frac{1}{2}\operatorname{erfc}\left[\sqrt{xv/(1+e)D}\right] + \int_{\frac{x}{(1+e)v}}^{\infty} g(s\,|\,t)(1)ds \approx g_a t\left[\frac{x}{(1+e)v}\right]^{-a/2},$$

the leading tail of $C_S(x,t)$ of (3) decays like $\frac{2}{a} g_a t v^{a/2} x^{-1-a/2}$.

Since neither mean nor variance exist, the observed mean and variance are dominated by the behavior of the solution on its leading tail. We can therefore for the purpose of estimating the observable mean and variance approximate the solution by its accompanying Pareto distribution as long as $L >> |v|(g_a t)^{2/a}$. Then

$$C(x,t) \approx \frac{a}{2}\frac{|v|^{a/2}\, g_a t}{x^{a/2+1}}\, c_{[|v|(g_a t)^{2/a},\infty)}(x),$$

where $g_a = 1/\Gamma(1-a/2)$ and $c_{[|v|(g_a t)^{2/a},\infty)}(x) = \begin{cases} 1 & \text{if } x > |v|(g_a t)^{2/a} \\ 0 & \text{else} \end{cases}$. Now it is a simple matter to estimate the observed mass, mean and variance over a fixed length scale.

Mass: $$\int_{|v|(g_a t)^{2/a}}^{L} C(x,t)dx \approx 1 - |v|^{a/2}\, g_a t / L^{a/2} \approx 1.$$

Mean:

$$\int_{|v|(g_a t)^{2/a}}^{L} x\cdot C(x,t)dx \approx \frac{a}{2}|v|^{a/2} g_a t \int_{|v|(g_a t)^{2/a}}^{L} x\cdot x^{-a/2-1}dx$$

$$= \frac{a}{2(1-a/2)}|v|^{a/2} g_a t\left\{L^{1-a/2} - \left[|v|(g_a t)^{2/a}\right]^{1-a/2}\right\}.$$

$$\approx \frac{a}{2-a}|v|^{a/2} g_a t L^{1-a/2}$$

Variance:

$$
\begin{aligned}
&\frac{a}{2}|v|^{a/2} g_a t \int_{|v|(g_a t)^{2/a}}^{L} x^{1-a/2}\,dx - \text{mean}^2 \\
&= \frac{a}{(4-a)}|v|^{a/2} g_a t \left\{ L^{2-a/2} - \left[|v|(g_a t)^{2/a} \right]^{2-a/2} \right\} - \text{mean}^2 \\
&\approx \frac{a}{4-a}|v|^{a/2} g_a t L^{2-a/2} - \left(\frac{a}{2-a}|v|^{a/2} g_a t L^{1-a/2} \right)^2 \\
&\approx \frac{a}{4-a}|v|^{a/2} g_a t L^{2-a/2}.
\end{aligned}
$$

These observations are consistent with numerical evaluations of observed mean and variance of solutions generated by (3).

ACKNOWLEDGEMENT

This research was supported by the U.S. Department of Energy, Basic Energy Sciences grant #DE-FG03-98ER14885, and National Science Foundation, Program of Hydrologic Sciences grant #EAR-9980484.

REFERENCES

Adams, E. E. and L. W. Gelhar, Field study of dispersion in a heterogeneous aquifer, 2, Spatial moments analysis, *Water Resour. Res.*, **28**(12), 3293-3307, 1992.

Balakrishnan, V., Fractional powers of closed operators and the semi-groups generated by them, *Pacific J. Math.*, **10**, 419-437, 1960.

Benson, D. A., The fractional advection-dispersion equation: Development and application, Ph.D. thesis, Univ. of Nevada, Reno, 1998.

Benson, D. A., R. Schumer, S. W. Wheatcraft, and M. M. Meerschaert, Fractional dispersion, Lévy motion, and the MADE tracer tests, in press, *Transport in Porous Media*, 2000a.

Benson, D. A., S. W. Wheatcraft, and M. M. Meerschaert, Application of a fractional advection-dispersion equation, *Water Resour. Res.*, **36**(6), 1403-1412, 2000b.

Benson, D. A., S. W. Wheatcraft, and M. M. Meerschaert, The fractional-order governing equation of Lévy motion, *Water Resour. Res.*, **36**(6), 1413-1423, 2000c.

Bertoin, J., *Lévy processes*, Cambridge University Press, Cambridge 1996.

Bochner, S., Diffusion equations and stochastic processes. *Proc. Nat. Acad. Sci. USA* **85**, 369-370, 1949.

Boggs, J.M. and E.E. Adams, Field study of dispersion in a heterogeneous aquifer, 4; Investigation of adsorption and sampling bias, *Water Resour. Res.*, **28**(12), 3325-3336, 1992.

Boggs, J.M., L.M Beard, S.E. Long, and M.P. McGee, Database for the second macrodispersion experiment (MADE-2), *EPRI report* TR-102072, Electric Power Res. Inst., Palo Alto, CA, 1993.

Brusseau, M., Transport of rate-limited sorbing solutes in heterogeneous porous media: Application of a one-dimensional multifactor nonideality model to field data, *Water Resour. Res.*, **28**(9), 2485-2497, 1992.

Chaves, A.S., A fractional diffusion equation to describe Lévy flights, *Phys. Lett. A*, **239**, 13-16, 1998.

Compte, A., Continuous time random walks on moving fluids, *Phys. Rev. E,* **55**(6), 6821-6831, 1997.

Cvetkovic V., and Dagan G., Transport of kinetically sorbing solute by steady random velocity in heterogeneous porous formations, *J. Fluid Mech.*, **265**, 189-215, 1994.

Feller, W., *An Introduction to Probability Theory and Its Applications, Volume II*, 2nd ed., John Wiley & Sons, New York, 1971.

Haggerty, R., and S. M. Gorelick, Multiple-rate mass transfer for modeling diffusion and surface reactions in media with pore-scale heterogeneity, *Water Resour. Res.*, **31**(10), 2383-2400, 1995.

Haggerty, R., S. A. McKenna, and L.C. Meigs, On the Late-Time Behavior of Tracer Test Breakthrough Curves, preprint,1999.

Harvey, C. and S.M.Gorelick, Rate-limited mass transfer or macrodispersion: Which dominates plume evolution at the Macrodispersion Experiment (MADE) site? *Water Resour. Res.*, **36**(3), 637-650, 2000.

Jury, W., Simulation of solute transport using a transfer function model, *Water Resour. Res.*, **18**(2)**,** 363-368, 1982.

Kanter, M., Stable densities under change of scale and total variation inequalities, *The Annals of Probability*, **3**(4), 697-707, 1975.

Klafter, J., M.F. Shlesinger, and G. Zumofen, Beyond Brownian motion, *Physics Today*, **49**(2), 33-39, 1996.

Meerschaert, M. M., D. A. Benson, and B. Bäumer: Multidimensional advection and fractional dispersion, *Phys. Rev. E,* **59**(5), 5026-5028, 1999.

Rehfeldt, K.R., Boggs, J.M., and Gelhar, L.W., Field study of dispersion in a heterogeneous aquifer. 3: Geostatistical analysis of hydraulic conductivity, *Water Resour. Res.*, **28**(12), 3309-3324, 1992.

Saichev, A. and G. Zaslavsky, Fractional kinetic equations: solutions and applications. *Chaos*, **7**(4), 753-764,1997.

Samorodnitsky, G. and M. S. Taqqu, *Stable Non-Gaussian Random Processes: Stochastic Models with Infinite Variance*, Chapman and Hall, New York, 1994.

Sato, K., *Lévy processes and infinitely divisible distributions*, Cambridge University Press, Cambridge, 1999.

Schumer, R., Benson, D., Meerschaert, M., and Wheatcraft, S, Eulerian derivation of the fractional advection-dispersion equation, in press, *J. Cont. Hyd.*, 2000.

Taylor, S., The measure theory of random fractals, *Math. Proc. Cambridge Philos. Soc.* **100,** 383 (1986).

van Genuchten, M. T., and P. J. Wierenga, Mass transfer studies in sorbing porous media, I, Analytical solutions, *Soil Sci. Soc. Am. J.*, **40**, 473-481, 1976.

FIGURE CAPTIONS

Figure 1. Graphs of completely skewed a/2-stable distributions. They are the blueprints for the distribution of operational time.

Figure 2. Log-log plot of the MADE-2 tritium mass distribution. The slope of the tail is used to determine the parameter a.

Figure 3. 1st moments of the linearized MADE-2 tritium mass distribution together with the moments adjusted for scale dependency.

Figure 4. 2nd moments of the linearized MADE-2 tritium mass distribution together with the moments adjusted for scale dependency.

Figure 5. Linear plots of the MADE-2 tritium mass distribution with model.

Figure 6. Semi-log plots of the MADE-2 tritium mass distribution with model.

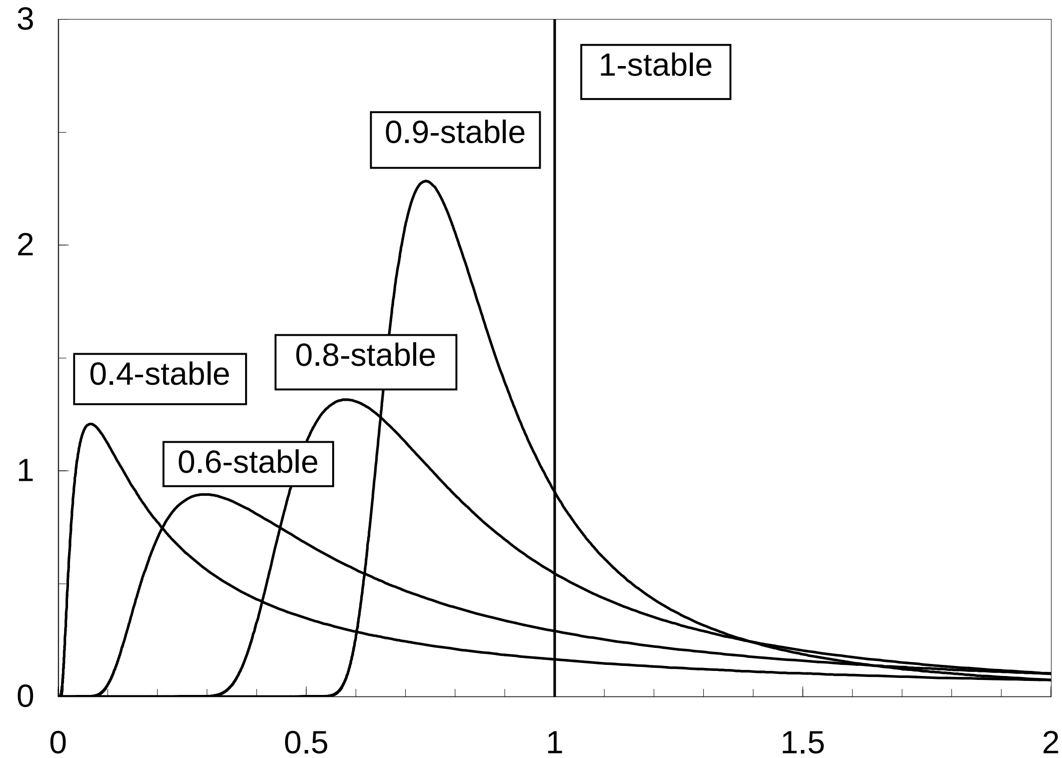
3
2
1
0
0
0.5
1
1.5
2
1-stable
0.9-stable
0.8-stable
0.4-stable
0.6-stable

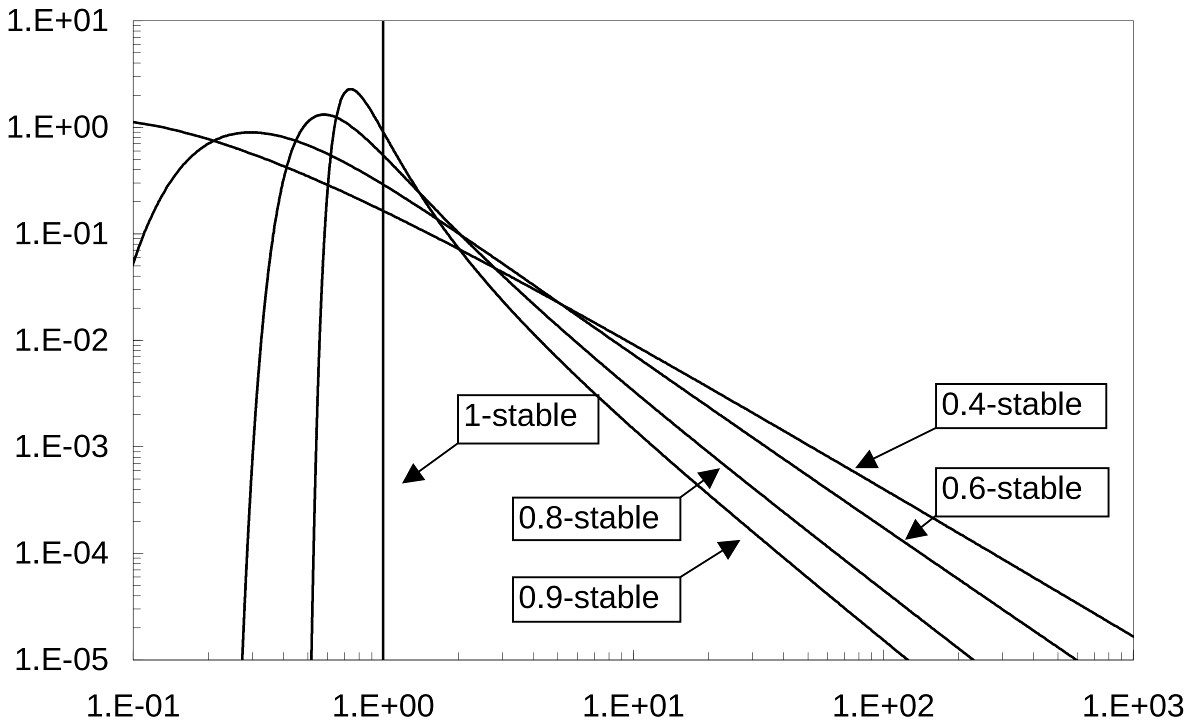
1.E+01
1.E+00
1.E-01
1.E-02
1.E-03
1.E-04
1.E-05
1.E-01
1.E+00
1.E+01
1.E+02
1.E+03
1-stable
0.4-stable
0.6-stable
0.8-stable
0.9-stable

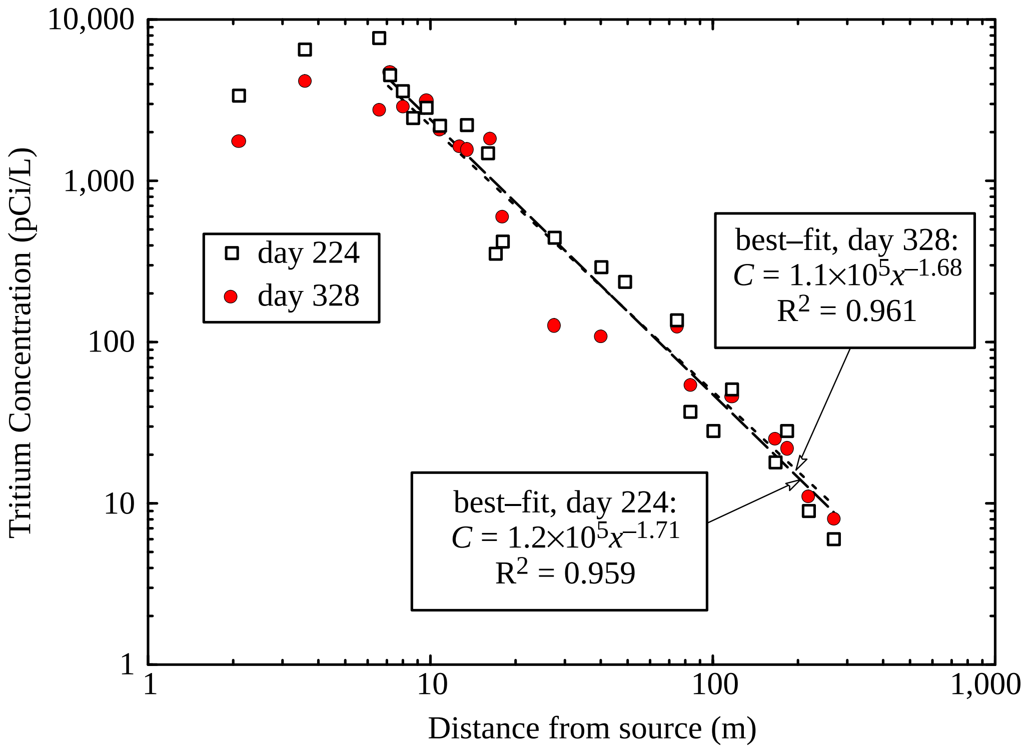
10,000
1,000
100
10
1
Tritium Concentration (pCi/L)
1
10
100
1,000
Distance from source (m)
day 224
day 328
best–fit, day 328:
C = 1.1×10^5 x^−1.68
R^2 = 0.961
best–fit, day 224:
C = 1.2×10^5 x^−1.71
R^2 = 0.959

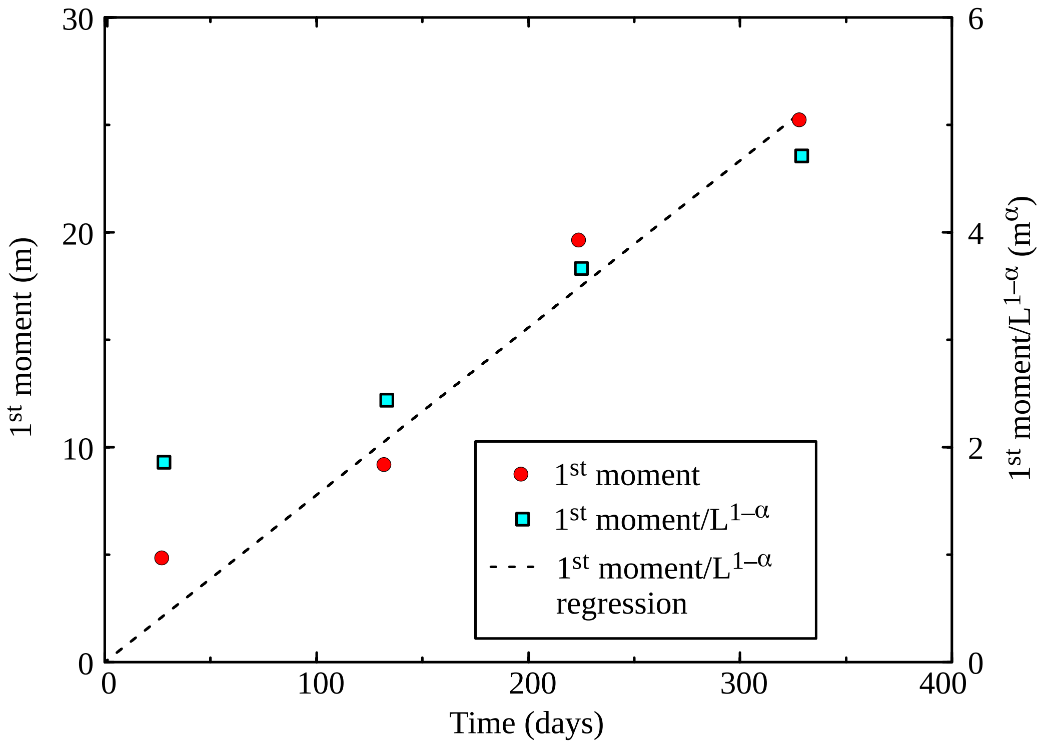

30
20
10
0
6
4
2
0
0
100
200
300
400
Time (days)
1st moment (m)
1st moment/L1–α (mα)
1st moment
1st moment/L1–α
1st moment/L1–α
regression

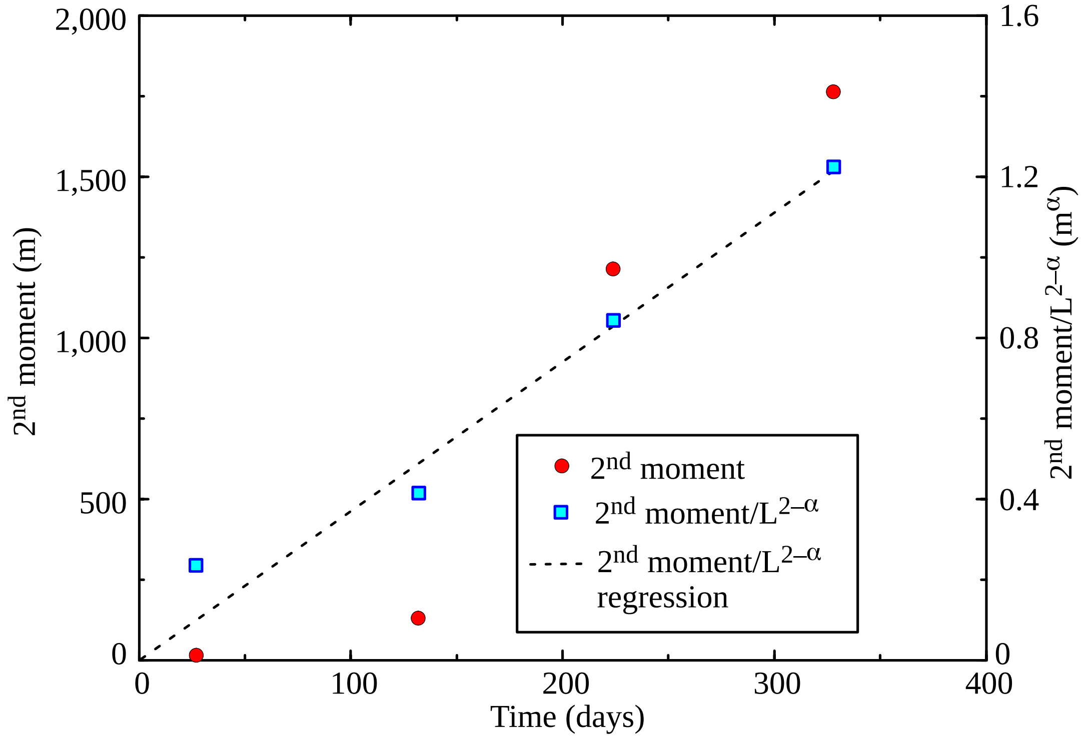
2,000
1,500
1,000
500
0
2^{nd} moment (m)
1.6
1.2
0.8
0.4
0
2^{nd} moment/$L^{2-\alpha}$ (m^{α})
0
100
200
300
400
Time (days)
2^{nd} moment
2^{nd} moment/$L^{2-\alpha}$
2^{nd} moment/$L^{2-\alpha}$ regression

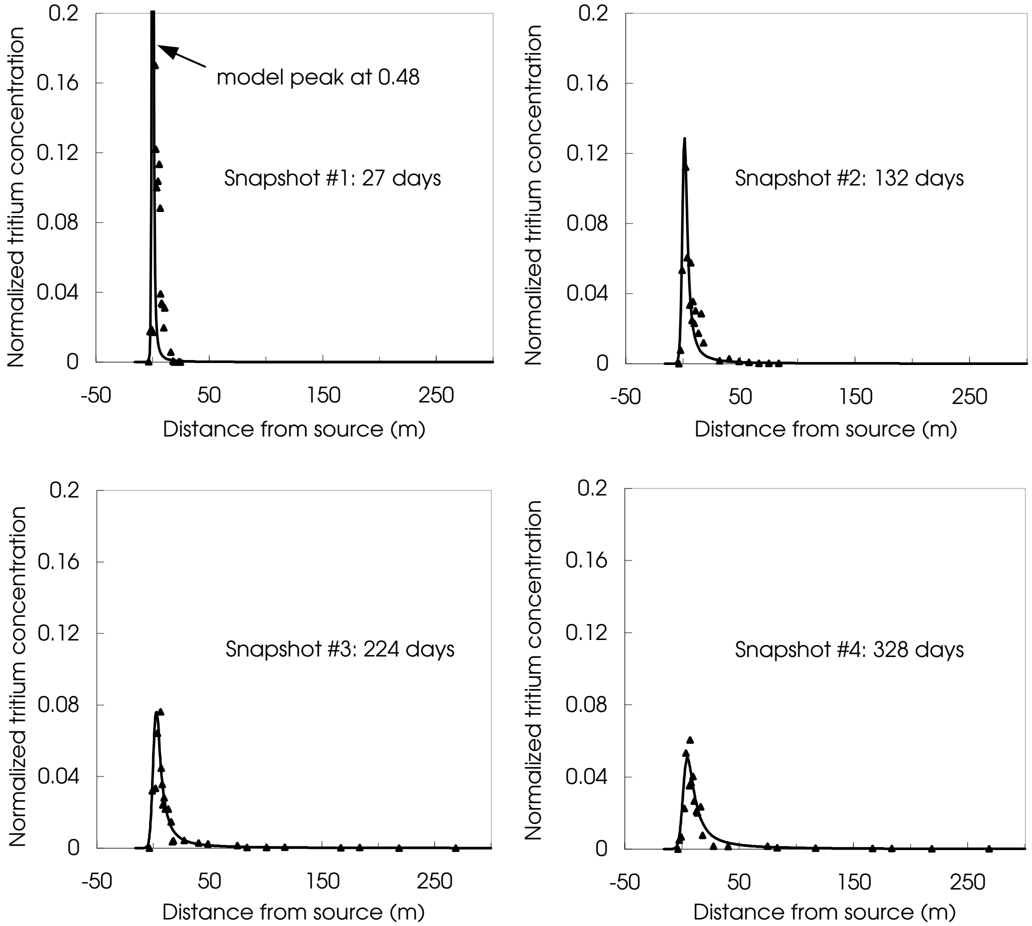

model peak at 0.48
Snapshot #1: 27 days
Snapshot #2: 132 days
Snapshot #3: 224 days
Snapshot #4: 328 days
Normalized tritium concentration
Distance from source (m)
0.2
0.16
0.12
0.08
0.04
0
-50
50
150
250

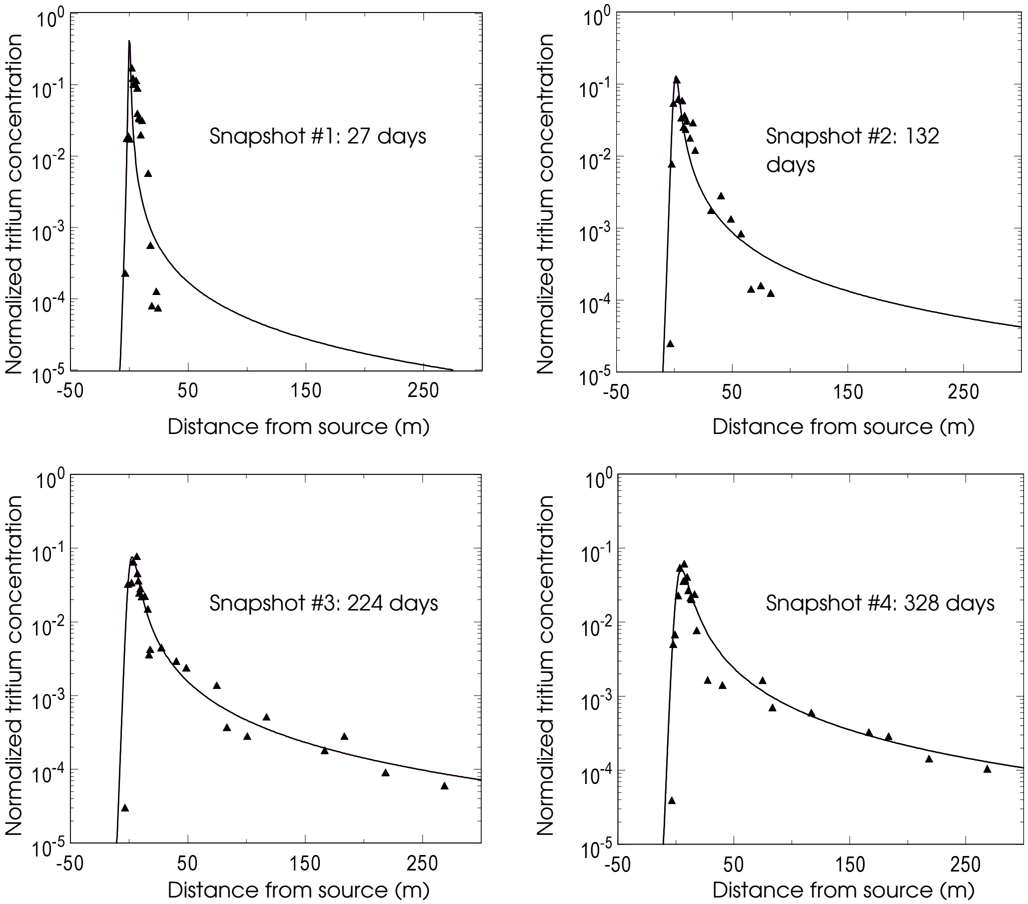

Snapshot #1: 27 days
Snapshot #2: 132 days
Snapshot #3: 224 days
Snapshot #4: 328 days
Normalized tritium concentration
Distance from source (m)
10^0
10^-1
10^-2
10^-3
10^-4
10^-5
-50
50
150
250